

Keep the Lights On, Keep the Lengths in Check: Plug-In Adversarial Detection for Time-Series LLMs in Energy Forecasting

Hua Ma^{*}, Ruoxi Sun^{*}, Minhui Xue^{*}, Xingliang Yuan[†], Carsten Rudolph[‡], Surya Nepal^{*}, Ling Liu[§]

^{*}CSIRO’s Data61, Australia

[†]The University of Melbourne, Australia

[‡]Monash University, Australia

[§]Georgia Institute of Technology, United States

Abstract

Accurate time-series forecasting is increasingly critical for planning and operations in low-carbon power systems. Emerging time-series large language models (TS-LLMs) now deliver this capability at scale, requiring no task-specific retraining, and are quickly becoming essential components within the Internet-of-Energy (IoE) ecosystem. However, their real-world deployment is complicated by a critical vulnerability: adversarial examples (AEs). Detecting these AEs is challenging because (i) adversarial perturbations are optimized across the entire input sequence and exploit global temporal dependencies, which renders local detection methods ineffective, and (ii) unlike traditional forecasting models with fixed input dimensions, TS-LLMs accept sequences of variable length, increasing variability that complicates detection. To address these challenges, we propose a *plug-in* detection framework that capitalizes on the TS-LLM’s own variable-length input capability. Our method uses sampling-induced divergence as a detection signal. Given an input sequence, we generate multiple shortened variants and detect AEs by measuring the consistency of their forecasts: Benign sequences tend to produce stable predictions under sampling, whereas adversarial sequences show low forecast similarity, because perturbations optimized for a full-length sequence do not transfer reliably to shorter, differently-structured subsamples. We evaluate our approach on three representative TS-LLMs (TimeGPT, TimesFM, and TimeLLM) across three energy datasets: ETTh2 (Electricity Transformer Temperature), NI (Hourly Energy Consumption), and Consumption (Hourly Electricity Consumption and Production). Empirical results confirm strong and robust detection performance across both black-box and white-box attack scenarios, highlighting its practicality as a reliable safeguard for TS-LLM forecasting in real-world energy systems.

Keywords

Internet of Energy, Time Series Forecasting, Adversarial Attacks

1 Introduction

As global power systems advance toward deep decarbonization, accurate forecasting of demand, renewable generation, and market signals has become central to maintaining flexibility, reliability, and economic efficiency. AI-enabled forecasting already improves predictive accuracy, adaptability, and uncertainty quantification in areas like scheduling, reserve procurement, and market operations [13, 57]. Similar progress in weather and climate modeling [65] highlights the broader potential of learning-based approaches.

This evolution aligns with a broader structural shift from centralized grid operations toward Internet-of-Energy (IoE) systems, characterized by dense sensing, heterogeneous data streams, and increasingly automated decision processes [71]. Modern IoE environments integrate high-resolution IoT meters, advanced metering infrastructure, and large fleets of distributed energy resources, producing massive volumes of time-series data describing load behavior, renewable output, asset conditions, and market behavior [12]. In such a distributed setting, machine learning has become essential for capturing nonlinear temporal dependencies and enabling real-time operational decisions beyond the reach of conventional tools. Practical adoption reflects this trend: smart-meter data supports load forecasting and anomaly detection [53], probabilistic renewable forecasts guide reserve activation and frequency control [17, 49], and data-driven analysis informs bidding optimization and manipulation detection [50].

Large language models (LLMs) are increasingly finding a role within this IoE landscape. Their ability to process natural language allows for operator-assistant tools that interpret free-form utility logs and alarms [33], and SCADA records, providing readable summaries and explanations for control-room decisions [24]. In electricity markets, foundation models help surface abnormal bidding behavior and potential manipulation [3]. At the distribution and residential scale, conversational LLM-based energy-management assistants translate user preferences into structured device-level actions [55]. LLM systems have also been explored for summarizing meteorological forecasts and interpreting wind and solar production patterns [34]. Together, these developments indicate that LLMs are becoming an integral component of monitoring, control, and market workflows across distributed energy systems. This deep integration makes LLM-based forecasting models increasingly critical for real-world IoE operations.

Although LLMs were originally developed for natural-language tasks, growing evidence shows that they generalize effectively to time-series data [21, 27, 37, 40, 61], delivering measurable gains in weather forecasting and energy-demand prediction [26, 28]. This capability, combined with their increasing use in IoE operations, has positioned LLMs as emerging general-purpose forecasters in real-world energy systems. Current adaptation approaches either repurpose pretrained language models through prompt engineering or train LLMs directly on large-scale time-series corpora with temporally aligned tokenization [35]. Commercial TS-LLMs such as TimeGPT [16], TimesFM [11], Chronos [4], and Moirai [66] follow this paradigm, providing strong zero-shot performance and enabling domain users across finance, healthcare, and energy management to obtain accurate forecasts through general-purpose APIs.

Their accelerating adoption within IoE workflows underscores the importance of ensuring that TS-LLM-based forecasting remains trustworthy and robust in operational settings.

Despite their rapid adoption, TS-LLM-based forecasting systems introduce significant challenges and new security risks. Unlike traditional models with fixed architectures and well-understood failure modes, TS-LLMs operate as large, opaque sequence learners whose outputs can be highly sensitive to input perturbations, data drift, and prompt variations [21, 27]. Recent studies show that they inherit the adversarial vulnerabilities of deep learning systems [26] and can exhibit unstable behavior under subtle input changes, distribution shifts, or numerical encoding biases [61]. These vulnerabilities become more pronounced in IoE settings, where data can be noisy, inconsistent across devices, and subject to real-time operational constraints. The difficulty is further heightened for commercial TS-LLMs, which are accessible only through fixed APIs and cannot be retrained or modified. Consequently, practical defenses must operate as modular, architecture-agnostic components that integrate seamlessly into existing TS-LLM forecasting pipelines without requiring access to model internals.

Motivated by these considerations, we examine the following key research question:

Is there an effective adversarial example defense that can be used as a plug-in for emerging TS-LLMs without requiring any prior knowledge of adversarial attacks?

To resolve this, we exploit a distinctive property of TS-LLMs that is absent in conventional deep learning models: their ability to process inputs of flexible length. Building on this characteristic, we design a detection mechanism for identifying adversarial time-series inputs. Our second insight concerns the nature of adversarial perturbations, which are optimized on the full input sequence. When an adversarial input x is randomly partitioned into equal-length subsamples x_{sub} and processed independently, the resulting forecasts diverge because perturbations tailored to the full sequence do not transfer reliably to the subsamples. Benign inputs lack such engineered modifications and therefore produce consistent forecasts across subsamples. This contrast forms the basis of our detection approach.

We summarize our main contributions as follows:

- To the best of our knowledge, this is the first work to develop countermeasures against adversarial example attacks on TS-LLMs [39]. We leverage the unique property of flexible input length in TS-LLMs to devise a length independence-based detection module (ILID) that can be used as a seamlessly plug-in without modifying the existing TS-LLM systems.
- ILID supports various sampling and thresholding strategies to distinguish adversarial from benign inputs. Notably, the threshold is computed solely from benign data, which enables generalizable detection and increases robustness against adaptive attacks due to the inherent randomness of the sampling process.
- We validate the effectiveness of ILID through extensive experiments on 3 energy benchmark datasets using TimeGPT, TimeLLM, and TimesFM. Our evaluation considers both practical black-box attacks and white-box attacks. Across all settings, the underlying TS-LLMs remain intact, demonstrating the modular design and practicality of our defense.

- Our evaluation focuses on black-box adversarial attacks to reflect realistic IoE conditions, and the method also demonstrates strong performance under white-box settings. We further show that adaptive thresholding can further improve detection accuracy.

2 Related Work

In this section, we introduce prior work on TS LLMs and on adversarial attacks and defenses relevant to time series forecasting.

2.1 Time Series LLMs

Existing approaches for enabling LLMs to perform time-series forecasting follow two main directions. The first adapts pretrained LLMs to numerical sequences. OFA [77] freezes most transformer layers and fine-tunes lightweight components for multiple forecasting tasks. PromptCast [70] formulates forecasting as prompt-based generation, while TEMPO [7] combines trend-seasonality-residual decomposition with soft prompt pooling. TEST [59] leverages contrastive learning to align time-series tokens with text prototypes and LLM4TS [9] aligns LLMs with temporal structure prior to parameter-efficient adaptation. These approaches, however, typically require nontrivial fine-tuning and depend on tokenization schemes not naturally suited to continuous signals. To reduce adaptation overhead, LLMTime [21] encodes values as digit strings to avoid training, and TimeLLM [27] introduces a lightweight re-programming module that maps time series into and out of LLM-compatible representations.

The second direction trains foundation models directly on large-scale time-series corpora. TimeGPT [16] was the first commercial model to demonstrate zero-shot forecasting, and Lag-LLaMA [51] extended this idea to probabilistic univariate prediction. More recent foundation models, including TimesFM [11], Chronos [4], and Moirai [66], further improve long-horizon forecasting and support flexible input and output lengths. By learning temporal structure from scratch, these TS-LLMs achieve strong zero-shot performance across multiple domains.

2.2 Adversarial Example Attacks and Defenses

Adversarial examples were first identified in image models [60], motivating extensive work on both white-box and black-box attacks. Gradient-based methods such as FGSM and BIM [31] dominate white-box settings, while black-box attacks typically rely on substitute models or evolutionary strategies [46, 58]. GAN-based techniques have also been explored for perturbation generation [56]. Although adversarial research in time series is comparatively limited, several studies have shown vulnerabilities in classification models: distance-based classifiers can be misled by crafted perturbations [45], and FGSM or BIM can markedly degrade deep time-series classifiers [14]. Subsequent work examined targeted and universal attacks [52] and developed substitute-model-based strategies [29]. Attacks on forecasting models remain less explored, with examples including perturbations to autoregressive predictors [10], gradient-based perturbations guided by importance metrics [67], and temporally targeted attacks [19]. Most recently, Liu et al. [39] proposed the first adversarial attack framework for TS-LLMs, highlighting the need for dedicated defenses.

Defensive strategies can be grouped into model modification, input transformation and adversarial detection. Model-level defenses primarily involve adversarial training [6, 44, 54, 64, 74] or architectural adjustments such as outlier classes [20]. These approaches increase computational cost, require access to attack examples and often degrade performance on benign inputs, which makes them impractical for LLMs that are expensive to retrain. Input-transformation defenses apply operations such as compression [41] or bit-depth reduction [22, 69], or reconstruct data through generative models [75]. While these techniques can suppress perturbations, they frequently reduce utility and are modality specific. Detection-based defenses analyze neighborhood characteristics [43] or train separate detectors [23], while others monitor internal layer consistency [42, 73] or examine prediction stability under input modifications [63, 69]. However, many detectors rely on adversarial examples during training and are susceptible to unseen attacks. Existing LLM-oriented defenses mostly target harmful-content filtering [30, 48, 68] and do not address vulnerabilities in numerical time-series forecasting.

3 Overview and Design of ILID

In this section, we first present a practical threat model for adversarial attacks in energy domain, then introduce our solution ILID to flag the adversarial samples.

3.1 Threat Model

The attacker may operate in either a black-box or white-box setting. As noted in recent work on TS-LLMs [39], the black-box setting is more realistic because commercial TS-LLMs such as TimeGPT are accessible only through APIs. White-box access becomes feasible when TS-LLMs are deployed locally, for example through open-source models on Hugging Face or internal fine-tuned models maintained by utilities or aggregators, where model weights, embeddings and tokenization schemes are fully exposed. Since existing AE attacks on TS-LLMs have been studied exclusively under black-box assumptions, we primarily focus on black-box attacks and include white-box evaluations (Section 4.5) for completeness.

This threat model is consistent with practical energy forecasting pipelines, where TS-LLM inputs often originate from external or partially trusted sources such as smart meters, IoT sensors, SCADA streams and third-party data feeds. Field evidence also shows that inverter telemetry and settings interfaces have exhibited software and configuration vulnerabilities in real deployments, allowing their measurement outputs to be altered or spoofed [5, 25, 72]. These channels are known to be susceptible to noise, tampering and data-integrity issues, which makes input-level perturbations a realistic attack surface even without model access.

The defender refers to the entity operating the TS-LLM forecasting system, such as a grid operator, an energy aggregator, a forecasting service provider, or even a local end user. The defender is assumed to have no prior knowledge of the adversarial example (AE) strategy and to possess only a small portion of benign data for setting and updating detection thresholds, consistent with prior AE detection work. The goal is to identify adversarial inputs while minimizing false positives. ILID is implemented as a lightweight plug-in module that neither modifies nor retrains the protected

TS-LLM, ensuring compatibility with both commercial and open-source forecasting workflows.

3.2 Overview

The design of ILID is illustrated in Figure 1. It is motivated by two key insights: the nature of adversarial example (AE) attacks and the unique characteristics of TS-LLMs. The first insight is that adversarial perturbations are highly input-dependent. Since they are carefully optimized with respect to specific inputs, the perturbations are tailored to reliably mislead the target model. The second insight concerns the inherent flexibility of TS-LLMs in handling input lengths. Unlike traditional forecasting models that require fixed input sizes, TS-LLMs can naturally accommodate variable input lengths. This property forms the foundation of ILID, enabling efficiency, effectiveness, and plug-in advantages in its design.

ILID operates in two phases: an offline phase and an online phase. In the offline phase, a small clean dataset \mathcal{X} is solely used to determine a similarity threshold, which is later employed for detecting AE inputs. Unlike a static threshold, ILID supports dynamic updates as detection proceeds. Since the online phase is straightforward, we focus below on the offline phase, with implementation details deferred to Section 3.3.

In the offline phase, the first step is to subsample each clean input \mathbf{x} of length T , producing multiple subsamples $\mathbf{x}_{\text{sub}i}$, $i \in (1, S)$, each with a reduced size (e.g., $T/2$). Next, these subsamples are fed into the underlying TS-LLM for inference, yielding predictions $\mathbf{y}_{\text{sub}i}$. Note that the length of $\mathbf{y}_{\text{sub}i}$ can be the same or different from the length of \mathbf{y} (the prediction corresponding to \mathbf{x}), but the outputs $\mathbf{y}_{\text{sub}i}$ are of the same length across $i \in (1, S)$. The third step is to compute the pairwise similarity among $\mathbf{y}_{\text{sub}i}$. For benign inputs, these predictions are expected to remain consistent with each other and with \mathbf{y} , since subsampling should not alter the temporal trend or forecasting tendency.

ILID applies these steps across all clean samples, producing a distribution of similarity scores. Based on this distribution and a predefined false rejection rate (FRR), ILID determines a threshold (Section 3.3) for online detection. During deployment, if an incoming input produces a similarity below this threshold, it is flagged as adversarial; otherwise, it is treated as benign.

3.3 Implementation

To be somewhat formal, following [39], we denote a time series at time t as \mathbf{x}_t , where $\mathbf{x}_{t,i}$ is the i -th component of this time series. Given a recent T historical observations $\mathbf{x}_{t-T+1:t}$, the TS-LLM predicts the future values for the subsequent τ time steps. The prediction is expressed as:

$$\tilde{\mathbf{y}}_{t+1:t+\tau} = \text{TS-LLM}(\mathbf{x}_{t-T+1:t}). \quad (1)$$

Note that the prediction horizon is typically less than or equal to the historical horizon, that is $\tau \leq T$. In following descriptions, we exchangeable use \mathbf{x} with \mathbf{x}_t and use \mathbf{y} with $\tilde{\mathbf{y}}$ for simplicity.

3.3.1 Subsampling. To sample the \mathbf{x} , the sampling strategy can be diverse or flexible. One simple sampling setting is to take one component in \mathbf{x} for every one component, similarly, to take two components for every two components. To ease understanding, we

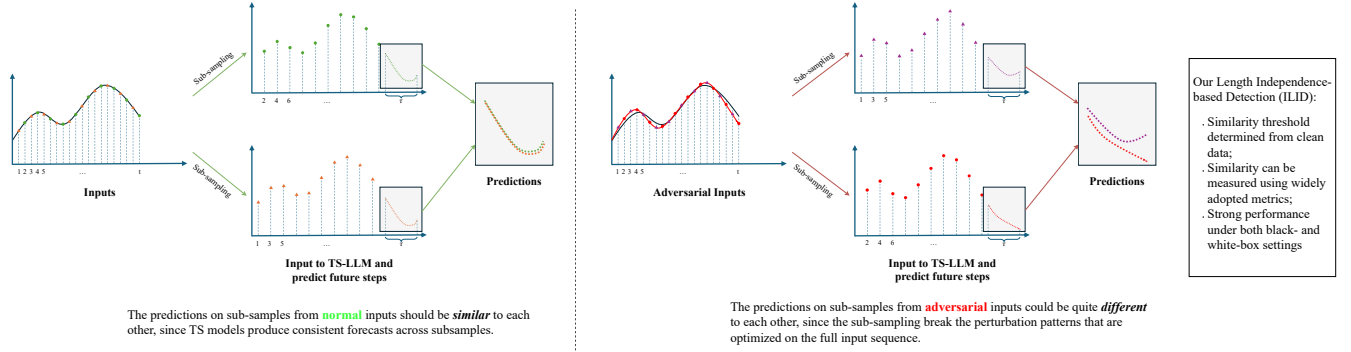


Figure 1: Overview.

take the first setting. Upon this setting, we have two subsamples

$$\mathbf{x}_{\text{sub},1} = \{\mathbf{x}_{t-T+1}, \mathbf{x}_{t-T+3}, \mathbf{x}_{t-T+5}, \dots, \mathbf{x}_{t-3}, \mathbf{x}_{t-1}\}$$

and

$$\mathbf{x}_{\text{sub},2} = \{\mathbf{x}_{t-T+2}, \mathbf{x}_{t-T+4}, \mathbf{x}_{t-T+6}, \dots, \mathbf{x}_{t-2}, \mathbf{x}_t\}.$$

Supposing that T is even, $\mathbf{x}_{\text{sub},1}$ corresponds to all odd components in \mathbf{x} , while $\mathbf{x}_{\text{sub},2}$ corresponds to all even components in \mathbf{x} .

We emphasize that the above example is only one sampling setting, while the sampling settings can vary according to the need. In addition, the components in each subsample do not necessarily need to be non-overlapping, as in the above example. More generally, the user can randomly take a fraction (e.g., 60%) of components from \mathbf{x} to form a subsample. Such inherent randomness in ILID enables it to defeat potential adaptive attacks, as we evaluate in Section 5.1.

3.3.2 Similarity. Given each subsample $\mathbf{x}_{\text{sub},i}$, a prediction with τ steps $\mathbf{y}_{\text{sub},i}$ is given through TS-LLM function. Suppose that we have S subsamples per \mathbf{x} , there will be S predictions. The pairwise similarity among these S predictions $\mathbf{y}_{\text{sub},i}$, $i \in (1, S)$ is computed. If we have N clean samples in \mathcal{X} , then the similarity of each $\mathbf{x} \in \mathcal{X}$ is computed. The similarity can be measured using widely adopted metrics, including Pearson similarity, as well as similarities derived from Euclidean distance and Manhattan distance. ILID is insensitive to the choice of similarity metric, as we show in Section 6.3, although we adopt Pearson similarity for extensive evaluations.

3.3.3 Threshold. To counter unseen AE attacks, ILID assumes no prior knowledge of attack strategies. The detection threshold is determined solely from the clean dataset. After computing the similarity of each clean sample in \mathcal{X} , we obtain N similarity values. We reasonably assume these values follow a normal distribution, from which the mean and standard deviation of the similarity distribution of benign inputs can be estimated. A false rejection rate (FRR), e.g., 1%, that can be tolerated is then preset. The FRR is the probability that a benign input is falsely regarded as adversarial, thus rejected. The corresponding percentile of the normal distribution is calculated and chosen as the detection threshold.

As an alternative, one may sort the N similarity values in ascending order and select the $(i+1)$ -th smallest value in the sorted list as the threshold, such that $\frac{i}{N} = \text{FRR}$ (e.g., $\text{FRR} = 1\%$). During online detection, if the similarity of a given input is lower than

this threshold, the input is regarded as adversarial; otherwise, it is treated as benign.

4 Experimental Evaluation and Results

In this section, we first describe the experimental setup, including the datasets and TS models used in our evaluation, then provide experimental results to showcase our detection performance against adversarial attacks.

4.1 Setup

In the context of energy applications, we identify three forecasting datasets for comprehensive evaluation, each reflecting practical scenarios in electricity load, generation, and consumption forecasting. Three TS-LLMs, namely TimeGPT, Time-LLM, and TimesFM, are considered. TimeGPT is a proprietary Nixtla model that requires payment per query, with limited free trials upon registration, and is available only through a black-box API. Although TimeLLM is open-source, its NeuralForecast library integration allows it to be used in a similar black-box fashion.

4.1.1 Datasets. We employ three energy application-specific datasets: Electricity Transformer Temperature Hourly (ETTh2), Hourly Energy Consumption Data (NI), and Hourly Electricity Consumption and Production (Consumption).

- **ETTh2** [76] contains different subsets for long-sequence time-series forecasting (LSTF). ETTh2 is one such subset, recorded at 1-hour resolution. Each entry includes the target variable “oil temperature” and six power load features. The dataset spans two years and is collected from two counties in China.

- **NI** [1] provides hourly energy consumption measurements in megawatts (MW), obtained from the official PJM repository. The Northern Illinois Hub (NI) is part of PJM Interconnection, a major regional transmission organization (RTO) in the United States. In our study, the NI dataset is used to examine regional power consumption patterns.

- **Consumption** [2] contains over six years of hourly electricity consumption and production data in Romania. It reports detailed generation by source—including nuclear, wind, solar, and others—offering insights into the country’s diverse energy mix. All values are measured in megawatts (MW).

Table 1: Forecasting performance of foundation models under clean and adversarial settings.

Dataset	Target	TimeGPT (Clean)			TimeGPT (AE)			TimeLLM (Clean)			TimeLLM (AE)			TimesFM (Clean)			TimesFM (AE)		
		MAE	MSE	R ²	MAE	MSE	R ²	MAE	MSE	R ²	MAE	MSE	R ²	MAE	MSE	R ²	MAE	MSE	R ²
ETTh2	OT	0.269	0.128	87.1%	0.345	0.203	79.6%	0.257	0.124	82.7%	0.368	0.237	66.9%	0.245	0.118	88.8%	0.324	0.181	82.8%
NI	NI-MW	0.282	0.196	78.4%	0.448	0.351	61.4%	0.480	0.414	71.0%	0.555	0.533	62.7%	0.257	0.182	77.4%	0.425	0.330	59.0%
Consumption	Consumption	0.154	0.050	93.6%	0.423	0.284	63.4%	0.403	0.293	69.4%	0.534	0.477	50.3%	0.208	0.107	88.3%	0.397	0.269	70.5%

4.1.2 *TS-LLMs*. Three TS-LLMs are employed for evaluation. TimeGPT and TimesFM perform zero-shot only forecasting on the above datasets.

- **TimeGPT** [16] is a commercial TS-LLM trained from scratch on a vast corpus of time series data. It is explicitly designed for time series forecasting, achieving high accuracy across diverse real-world applications. TimeGPT requires a subscription for usage. For example, the \$99/month standard plan permits 10,000 API calls per month, which we have subscribed to for experiments.

- **Time-LLM** [27] reprograms a pretrained LLM for general time series forecasting while keeping the language model, originally trained on textual corpora, unchanged. A key component is the Prompt-as-Prefix (PaP) strategy, which improves contextual understanding and guides the model toward accurate forecasting on reformatted time series data. To be user-friendly, Time-LLM has incorporated this PaP into its system prompt, where the user does not need to provide and can use the Time-LLM for forecasting. Time-LLM is integrated into the NeuralForecast library, making it straightforward to use in practice.

- **TimesFM** [11] is a pretrained time-series forecasting foundation model developed by Google Research, trained on 100 billion real-world time points. The public model from Hugging Face is able to be loaded and used directly, without additional fine-tuning. TimesFM-2.0-500M is used in our experiment.

4.2 Adversarial Example Attack

There is only one recent adversarial example (AE) attack, namely Directional Gradient Approximation (DGA) [39], specifically devised against TS-LLMs in a realistic black-box setting. Therefore, our evaluations primarily focus on this attack, while we defer evaluations of white-box attacks such as FGSM, BIM, and PGD to Section 4.5. The forecasting performance of TS-LLMs is assessed using three metrics: Mean Absolute Error (MAE), Mean Squared Error (MSE), and the R^2 score. The objective of an AE attack is to deviate the prediction from its normal output, such that MAE and MSE increase notably, while R^2 decreases. Note that if the performance deviation is marginal, the AE attack cannot be regarded as successful.

We apply DGA to all three datasets against each of the three TS-LLMs. Table 1 summarizes TS-LLM performance under both clean and adversarial example queries. We ensure that the attacks succeed before evaluating the defensive effect of ILID. As expected, both MAE and MSE exhibit a marked increase under AE queries compared to clean sample queries, whereas the R^2 score demonstrates a noticeable decline as expected.

4.3 Offline Similarity Threshold

To be comprehensive, we employ different sampling strategies to generate subsamples with three subsample sizes: 240, 160, and 120 time steps (input length), given the same query input \mathbf{x} with

$T = 480$ time steps. For the 240-step sampling, we take all odd and even components in \mathbf{x} , respectively, as subsamples, resulting in two subsamples per input sample under this setting. For the 160-step sampling, we subsample \mathbf{x} by selecting one element every three steps (i.e., with a stride of 3), respectively, as subsamples, resulting in three subsamples per input sample under this setting. For the 120-step sampling, subsamples are generated from input \mathbf{x} by selecting one element every four time steps, corresponding to a stride of 4, resulting in four subsamples per input sample under this setting.

Afterward, the pairwise similarity of the forecasting values from subsamples of the same size is computed and then used to determine the threshold based on the similarities of all retained clean samples in \mathcal{X} . The similarity distributions for clean queries under subsample lengths of 240, 160 and 120 in the ETTh2 dataset are shown in Figure 2 (top row). Here, the smallest mean pairwise similarity value is tolerated, while the second-smallest value is regarded as the threshold. More specifically, in Figure 2a, the threshold is set to 0.915, corresponding to tolerating one false positive.

It is worth noting that this threshold, although initially determined offline, does not need to remain static; it can be updated dynamically during online detection, as detailed in Section 6.2.

4.4 Online Detection Results

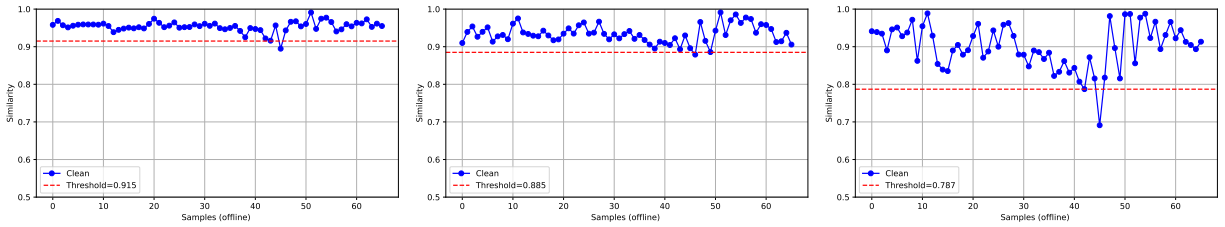
The dataset in all experiments is split into two equal parts; the first part is used to determine the offline threshold as detailed above, while the remaining samples are for online evaluation.

4.4.1 *TimeGPT*. We evaluate TimeGPT with all three datasets: ETTh2, NI and Consumption.

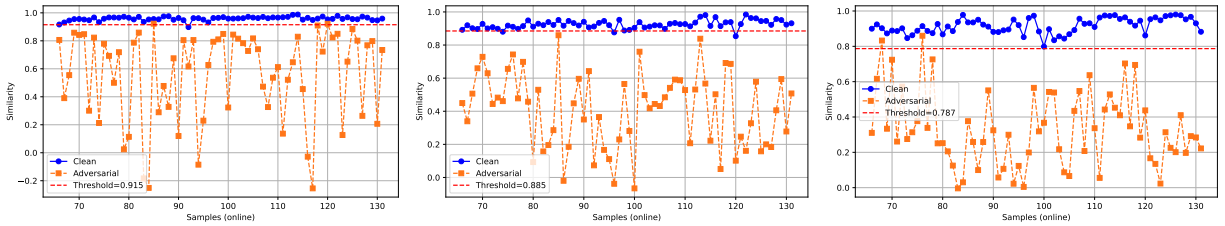
- *ETTh2*. The total number of ETTh2 samples is 132, each with 480 timesteps. Each sample is used to forecast the next 48 timesteps. The first 66 samples are used for threshold determination, while the remaining 66 samples are employed for online evaluation.

When the subsample length is 240 timesteps, the threshold is 0.915, as shown in Figure 2a. Similarly, the threshold is 0.885 in Figure 2b with a subsample length of 160 timesteps, and 0.787 in Figure 2c with a subsample length of 120 timesteps. In all cases, the threshold is determined by tolerating one false positive (as detailed in Section 4.3).

The bottom subfigures in Figure 2 present the corresponding online detection results based on the preset thresholds. In Figure 2d, with a subsample length of 240 timesteps, only one clean sample has a Pearson similarity below the threshold of 0.915 (blue), while two adversarial samples have Pearson similarities above it (orange). This indicates that one clean sample and two adversarial samples fail to be correctly detected when using the offline-determined threshold of 0.915. Figures 2e and 2f show the detection results when subsample lengths are 160 and 120 timesteps, respectively.



(a) Offline: subsample length = 240 (ETTh2) (b) Offline: subsample length = 160 (ETTh2) (c) Offline: subsample length = 120 (ETTh2)



(d) Online: subsample length = 240 (ETTh2) (e) Online: subsample length = 160 (ETTh2) (f) Online: subsample length = 120 (ETTh2)

Figure 2: Offline (top) and online (bottom) detection results for ETTh2 using TimeGPT with different subsample lengths.

More specifically, the FRR and FAR are detailed in Table 2. The preset FRR is 1.5% across all subsample lengths. For online detection, when the subsample length is 240 timesteps, the online FRR for clean samples remains at 1.5%, while the FAR for adversarial samples is 3.0%. With a subsample length of 160 timesteps, the online FRR increases to 4.5%, while the FAR is 0%. For a subsample length of 120 timesteps, the FRR is 0% and the FAR rises to 3.0%. The slight discrepancy between the preset FRR and the online FRR is potentially due to the small number of testing samples. Nevertheless, the differences are minor and acceptable.

- *Consumption*. The Consumption dataset consists of 164 samples, each with 720 timesteps, used to forecast the next 36 hours. As shown in Figure 3, the offline preset thresholds are 0.887, 0.770, and 0.692 when the subsample length is 360, 240, and 180 timesteps, respectively. The FRR and FAR results are summarized in Table 2. With an offline tolerance FRR of 1.2% for all subsample lengths, the online FRR for clean samples is 0% in all cases, while the FAR for adversarial samples is 7.3% (360 timesteps), 3.7% (240 timesteps), and 6.1% (180 timesteps).

- *NI*. The NI dataset consists of 268 samples, each with 480 timesteps, used to forecast the subsequent 48 timesteps. As shown in Figure 4, the offline thresholds are 0.924 for a subsample length of 240, 0.856 for a subsample length of 160, and 0.894 for a subsample length of 120. The FRR and FAR results are summarized in Table 2. With the same preset FRR of 0.7% across all subsample lengths, the FRR for clean samples and the FAR for adversarial samples are both 4.5% when the subsample length is 240 timesteps. For a subsample length of 160 timesteps, the FRR for clean samples is 5.2% and the FAR for adversarial samples is 2.2%. For a subsample length of 120 timesteps, both the online FRR for clean samples and the FAR for adversarial samples are 0.7%.

4.4.2 *TimeLLM*. Figure 5 shows the detection performance using TimeLLM on all three datasets. The ETTh2 dataset consists of 138 samples, each with 168 timesteps to forecast the next 24. A subsample length of 56 is selected, with a sampling stride of three timestep.

Table 2: Detection performance on three datasets (ETTh2, Consumption, and NI) using TimeGPT.

Dataset	Length	Threshold	Offline		
			FRR	FRR	FAR
ETTh2	240	0.915	1.5%	1.5%	3.0%
	160	0.885	1.5%	4.5%	0.0%
	120	0.787	1.5%	0.0%	3.0%
Consumption	360	0.887	1.2%	0.0%	7.3%
	240	0.770	1.2%	0.0%	3.7%
	180	0.692	1.2%	0.0%	6.1%
NI	240	0.924	0.7%	4.5%	4.5%
	160	0.856	0.7%	5.2%	2.2%
	120	0.894	0.7%	0.7%	0.7%

As shown in Figure 5a, the offline threshold is 0.852 with a preset FRR of 1.4%, determined using the first 69 samples. In Figure 5d, five clean samples fall below the threshold (blue), resulting in an online FRR of 7.2%, while six adversarial samples fall above the threshold (orange), corresponding to a FAR of 8.7%.

The Consumption contains 198 samples, each with 720 timesteps to forecast the next 24. A subsample length of 240 is chosen, with a sampling stride of three timesteps. As shown in Figure 5b, the offline threshold is 0.842 with a preset FRR of 1.0%. In Figure 5e, one clean sample falls below the threshold and two adversarial samples fall above it, corresponding to an online FRR of 1.0% and a FAR of 2.0%.

The NI dataset consists of 213 samples, each with 720 timesteps to forecast the following 24. A subsample length of 180 is used, with a sampling stride of four timesteps. Using the first 100 samples, the threshold is set to 0.908, as shown in Figure 5c, with a preset FRR of 1.0%. In Figure 5f, four clean samples and one adversarial sample fail to be correctly detected, corresponding to an online FRR of 3.5% and a FAR of 0.9%. For all three datasets, the FRR and FAR results are further summarized in Table 3.

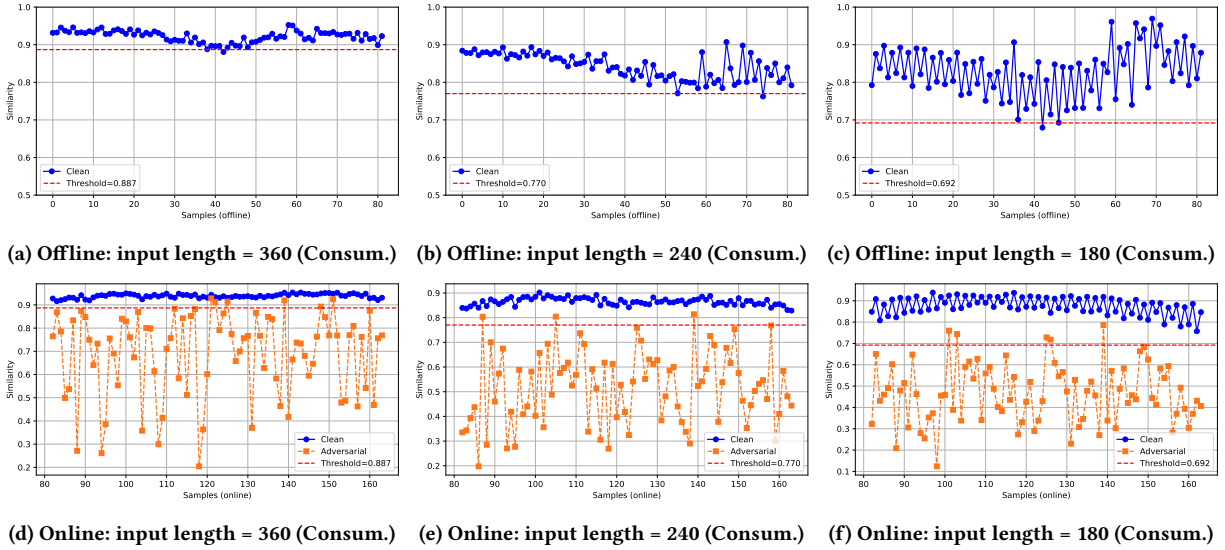


Figure 3: Offline (top) and online (bottom) detection results for Consumption using TimeGPT with different subsample lengths.

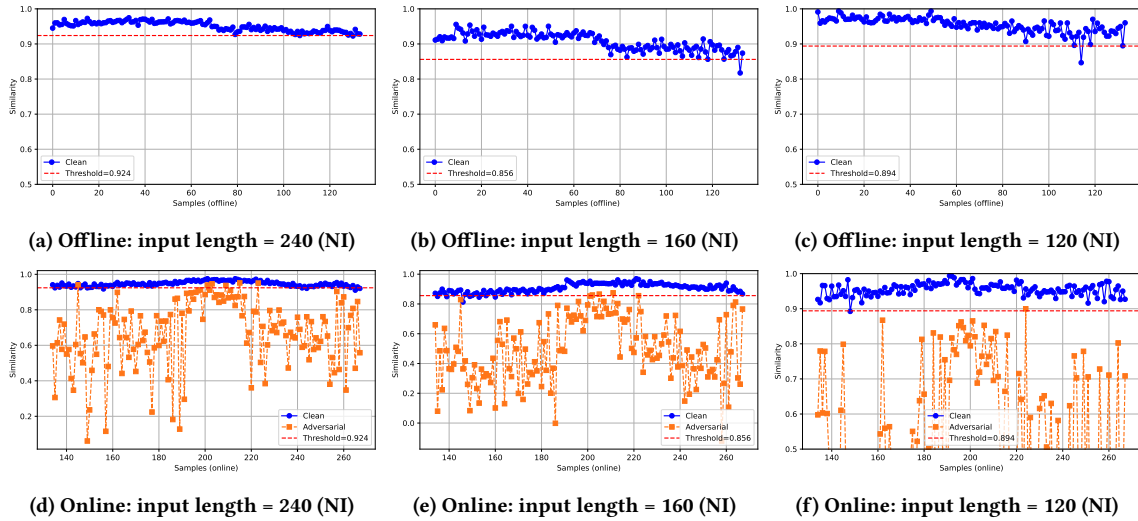


Figure 4: Offline (top) and online (bottom) detection results for NI using TimeGPT with different subsample lengths.

Table 3: Detection performance with TimeLLM.

Dataset	Length	Threshold	Offline		Online	
			FRR	FAR	FRR	FAR
ETTh2	56	0.852	1.4%	7.2%	8.7%	
Consumption	240	0.842	1.0%	1.0%	2.0%	
NI	180	0.908	1.0%	3.5%	0.9%	

Table 4: Detection performance with TimesFM.

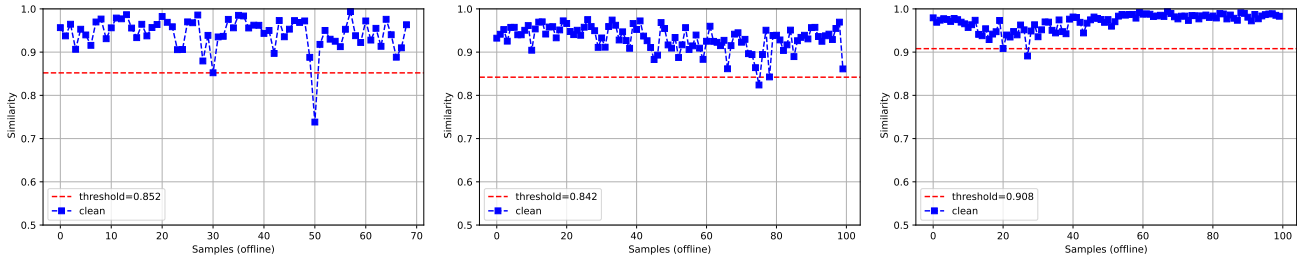
Dataset	Length	Threshold	Offline		Online	
			FRR	FAR	FRR	FAR
ETTh2	85	0.752	1.0%	2.9%	1.9%	
Consumption	85	0.804	1.0%	0.0%	0.0%	
NI	85	0.913	1.0%	3.9%	1.0%	

4.4.3 *TimesFM*. For this evaluation, all sample sizes of the ETTh2, Consumption, and NI datasets are set to 256 timesteps to forecast the future 48 timesteps. The subsample length is chosen to be 85 by applying stride-sampling with a stride of 2, starting respectively from the 2nd, 3rd, and 4th elements, rendering 3 subsamples.

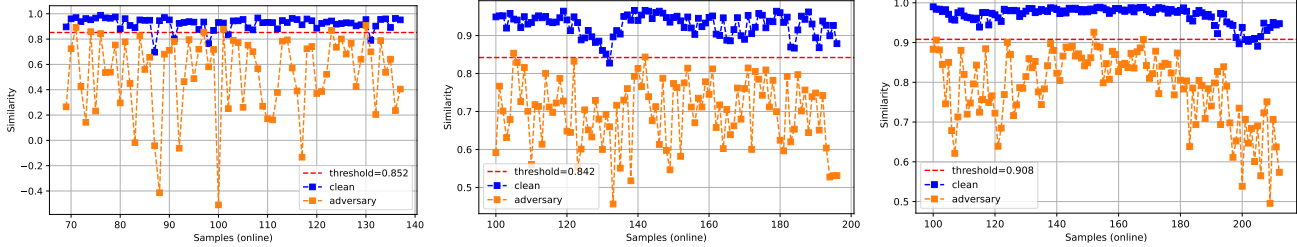
The top row of Figure 6 shows the offline-determined thresholds, while the bottom row presents the corresponding online detection results for both adversarial and clean samples. The detailed FRR and FAR results are summarized in Table 4. The preset FRR for all

datasets is 1.0%. The thresholds for ETTh2 and Consumption are 0.752 and 0.804, respectively, while the threshold for NI is 0.910.

For ETTh2, the online FRR for clean samples is 2.9%, with three samples failing to be correctly detected, and the FAR for adversarial samples is 1.9%. For the Consumption dataset, both FRR and FAR are 0.0%, indicating that all clean and adversarial samples are successfully detected. For the NI dataset, the online FRR is 3.9% and the FAR is 1.0%.

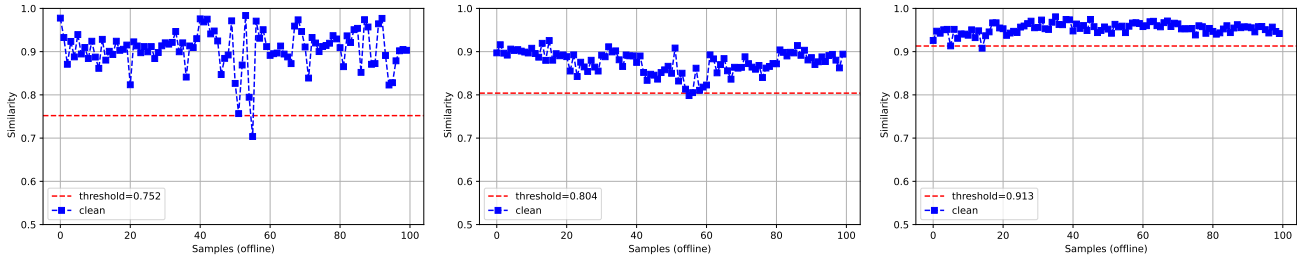


(a) Offline: subsample length = 56 (ETTh2) (b) Offline: subsample length = 240 (Consum.) (c) Offline: subsample length = 180 (NI)

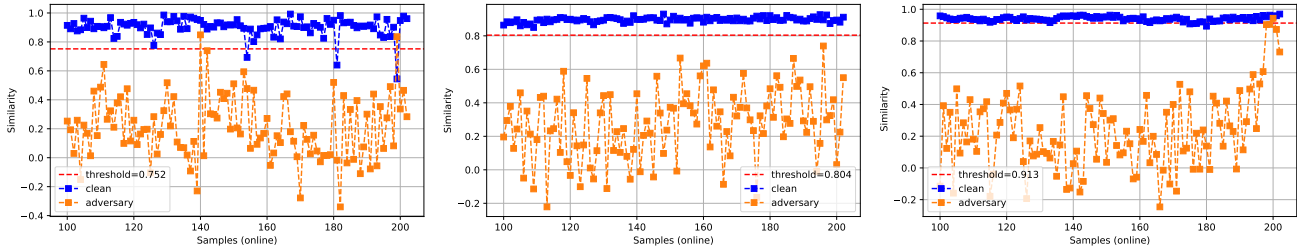


(d) Online: subsample length = 56 (ETTh2) (e) Online: subsample length = 240 (Consum.) (f) Online: subsample length = 180 (NI)

Figure 5: Offline (top) and online (bottom) detection results for TimeLLM across different datasets.



(a) Offline: subsample length = 85 (ETTh2) (b) Offline: subsample length = 85 (Consum.) (c) Offline: subsample length = 85 (NI)



(d) Online: subsample length = 85 (ETTh2) (e) Online: subsample length = 85 (Consum.) (f) Online: subsample length = 85 (NI)

Figure 6: Offline (top) and online (bottom) detection results for TimesFM across different datasets.

4.5 White-Box Adversarial Example Attacks

For all previous evaluations, we extensively experimented on black-box adversarial example attacks, which are most realistic in real world. Now we take the white-box AE attacks into account. The white-box attacks require access to the underlying TS-LLM, which is possible when the TS-LLM is a public model or the attacker is an insider. A targeted AE attack aims to force the model to predict a specific (incorrect) value, whereas an untargeted attack seeks to cause the model to output any value different from ground-truth [8,

15, 47]. In practical time-series forecasting, the true future values are usually unavailable to the attacker; thus, we assume the adversary cannot access the forecasting ground truth, following [39]. Under this assumption, we adopt a targeted attack and set the target value to 0, optimizing perturbations to reduce forecasting accuracy.

Three white-box AE attacks of FGSM [18], BIM [31], and PGD [44] are adopted. It is worth mentioning that none of these AE attacks has been mounted on TS-LLMs so far. TimesFM is used for experiments because it is publicly accessible from Hugging Face, while we use the NI dataset.

Table 5: TimesFM forecasting performance w/wo *white-box* adversarial example attack (NI dataset on TimesFM). - means that it is the same as the first row.

Attack Method	Clean Samples			Adversarial Samples		
	MAE	MSE	R ²	MAE	MSE	R ²
DGA (Black)	0.257	0.182	77.4%	0.425	0.330	59.0%
FGSM (White)	-	-	-	0.534	0.454	43.5%
BIM (White)	-	-	-	0.651	0.628	21.8%
PGD (White)	-	-	-	0.665	0.673	16.1%

Table 6: Detection performance with *white-box* adversarial example attack (NI dataset on TimesFM).

Attack Method	Offline		Online	
	FRR	FRR	FAR	FAR
DGA (Black)	1%	3.9%	1%	1%
FGSM (White)	1%	3.9%	0%	0%
BIM (White)	1%	3.9%	0%	0%
PGD (White)	1%	3.9%	1%	1%

As in the black-box setting, a perturbation scale of 0.2 is adopted to perform white-box AE attacks. The attack performance is shown in Table 5, which also includes the DGA black-box attack for comparison. The metrics of MAE, MSE, and R² are used to evaluate the attack effect. Both MAE and MSE gradually increase for FGSM, BIM, and PGD, while the R² score decreases significantly. Based on the same setting, the attack effect strengthens from FGSM to PGD, consistent with the expectation that white-box attacks typically exhibit stronger performance than black-box attacks.

ILID is then applied to detect white-box AEs. The FAR and FRR results are detailed in Table 6. The subsample length is 85 timesteps, with the original sample length set to 256 timesteps to forecast next 48 timesteps. The offline threshold is 0.913, corresponding to a preset FRR of 1%. The online FRR is 3.9%. For adversarial detection, the online FAR is 0% for both FGSM and BIM, and 1% for PGD.

5 Adaptive Attacks

In an adaptive attack, the adversary has full knowledge of the specific defense. However, ILID incorporates inherent randomness that complicates such adaptive attacks. This randomness arises from three sources: subsample length, the specific sampling setting (e.g., stride/window), and the particular subsamples used. The attacker cannot control these random choices. Note that in the previous section, in some cases, we have intentionally varied subsample length and sampling settings across datasets and TS-LLMs; those experiments show that ILID remains largely effective despite such parameter changes, which helps harden against adaptive strategies. Below, we evaluate ILID more deliberately by introducing randomness while keeping the *same* NI dataset and the *same* TS-LLM of TimesFM. We then test ILID against an adaptive attack, the sparse adversarial attack [38], which crafts adversarial examples by perturbing only a fraction of timesteps on the TS-LLM.

5.1 Sampling Strategy

For a given input length, different random sampling strategies and settings can result in varying subsample lengths. Once such randomness is determined by the defender, it remains fixed, similar

Table 7: Detection performance under varying subsample sizes (NI and TimesFM).

Subsample Size	Threshold	# of Offline		# of Online	
		FRR	FRR	FAR	FAR
153	0.860	1.0%	1.9%	3.9%	3.9%
128	0.878	1.0%	1.0%	6.8%	6.8%
85	0.913	1.0%	3.9%	1.0%	1.0%
64	0.794	1.0%	5.8%	1.9%	1.9%

Table 8: Threshold and detect results with the different number of pairwise similarity scores (Consumption dataset on TimeGPT).

The Number	Threshold	# of Offline		# of Online	
		FRR	FRR	FAR	FAR
1	0.940	1.2%	0%	1.2%	1.2%
2	0.912	1.2%	0%	1.2%	1.2%
3	0.843	1.2%	0%	1.2%	1.2%
4	0.836	1.2%	0%	0.0%	0.0%
5	0.775	1.2%	0%	2.4%	2.4%
6	0.692	1.2%	0%	6.1%	6.1%

to setting a random seed, to ensure reproducibility. In Table 7, the input sample length is 256 timesteps, while the resulting subsample lengths are 153, 128, 85, and 64. As shown in the table, the offline-determined thresholds are 0.860, 0.878, 0.913, and 0.794 for subsample lengths of 153, 128, 85, and 64, respectively. Figure 7 then provides a more detailed breakdown of the results for the subsample lengths of 128, 85, and 64.

The defender can randomly choose any of these sampling strategies and apply the corresponding threshold for online detection, as long as it uses the same random seed for sampling. In all cases, the FRR is less than 5.8% and the FAR is below 6.8%. This indicates that an adaptive attacker cannot predict which sampling strategy will be adopted for defense.

5.2 Used Subsamples

Even when the subsample length is fixed, the number of subsamples used to determine the threshold can be chosen randomly. In Table 8, the subsample length is fixed at 180 (from an original input length of 720). Four subsamples of length 180 are generated by taking one sample every three steps, starting from the 1st, 2nd, 3rd, and 4th positions, respectively. The pairwise similarity among these subsamples is then calculated to set the threshold. A single round of comparison among the four subsamples yields $\binom{4}{2} = 6$ pairwise similarity scores.

The threshold can be determined by averaging any selected subset of these six pairwise similarity scores, allowing flexible aggregation strategies. Table 8 presents an example where different numbers of pairwise similarity scores (from 1 to 6) are used. In all cases, the online detection achieves an FRR of 0.0% with a maximum FAR of 6.1%. The total number of possible combinations when selecting at least one pairwise similarity score is: $\sum_{k=1}^6 \binom{6}{k} = 2^6 - \binom{6}{0} = 64 - 1 = 63$.

This indicates that an attacker faces significant uncertainty, as the defender can flexibly choose different subsets of pairwise similarity scores to compute thresholds for detection.

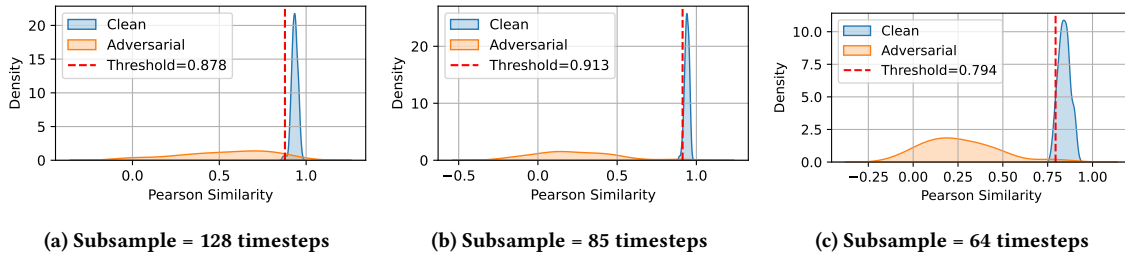


Figure 7: The online similarity distribution across varying subsample sizes (NI on TimesFM). It shows that there exists a small overlap between two FRR and FAR.

Table 9: TimesFM forecasting performance w/wo attack.

Dataset	Target	Clean query			AE query		
		MAE	MSE	R ²	MAE	MSE	R ²
NI	NI-MW (normal)	0.257	0.182	77.4%	0.425	0.330	59.0%
NI	NI-MW (sparse)	0.257	0.182	77.4%	0.403	0.311	61.2%

Table 10: Detection performance with sparse attack (NI and TimesFM).

Subsample Size	Threshold	# of Offline		# of Online	
		FRR	FRR	FRR	FAR
64 (normal)	0.794	1.0%	5.8%	1.9%	
64 (sparse)	0.794	1.0%	5.8%	1.0%	

5.3 Sparse Adversarial Attack

In the latest sparse adversarial attack [38], perturbations are added only to a fraction of the input timesteps rather than the full sequence. This can be regarded as an adaptive attack to bypass one of ILID core insights that adversarial perturbations are optimized over the entire input space.

In our sparse implementation, 40% of the input timesteps are perturbed, while the rest timesteps remain intact. For a fair comparison, we ensure that the sparse adversarial attack achieves a similar (though slightly lower) attack effect as the normal attack, where latter all timesteps are perturbed. As shown in Table 9, the sparse attack yields an MAE of 0.403, an MSE of 0.311, and an R² of 61.2%.

For ILID, the subsample length is set to 64 by uniformly selecting one data point every four timesteps from the original sequence. The offline threshold is determined based on a preset FRR of 1%. The corresponding online detection results are an FRR of 5.8% and a FAR of 1.0%, as reported in Table 10.

In a nutshell, under the same setting and comparable attack effect, the detection performance of ILID on sparse adversarial attacks is slightly better (with a 0.9% decrease in FAR) than on normal attacks. The primary reason is that the perturbation weight per timestep in sparse attacks is higher than in normal attacks; therefore, randomly removing such perturbed timesteps leads to lower similarity among subsamples, making detection easier.

6 Discussion

In this section we further discuss several factors that may influence the performance of ILID during deployment.

Table 11: Detection performance at different FRR tolerances (Ethh2 and TimesFM).

Subsample Size	Threshold	# of Offline		# of Online	
		FRR	FRR	FRR	FAR
128	0.834	1.0%	1.9%	8.7%	
-	0.851	2.0%	3.9%	7.8%	
-	0.885	3.0%	5.8%	2.9%	

6.1 FRR vs FAR

FRR refers to the tolerable false rejections of benign samples and is preset in advance. Importantly, there exists a trade-off between FRR and FAR. In security-critical applications, one may sacrifice some user experience in order to suppress FAR, which can be flexibly achieved by adopting a higher preset FRR when determining the detection threshold.

To evaluate this trade-off between FRR (usability) and FAR (security), the preset FRR is varied at 1.0%, 2.0%, and 3.0% to determine the threshold and evaluate the online detection results. TimesFM is used for evaluation on the ETTh2 dataset. For each sample with length 256 forecasting the next 48 timesteps, the subsample length is set to 128 timesteps. The detection performance of ILID is summarized in Table 11 and illustrated in Figure 8. When the offline FRR is set to 1.0%, the online detection achieves an FRR of 1.9% and an FAR of 8.7%. Increasing the preset FRR to 2.0% leads to a slight rise in the online FRR to 3.9%, while the FAR decreases to 7.8%. Further raising the preset FRR to 3.0% results in an online FRR of 5.8% and a reduced FAR of 2.9%. These results confirm that tolerating a slightly higher FRR can significantly reduce FAR.

6.2 Dynamic Threshold

When an incoming sample is classified as benign under the online detection, its corresponding similarity can be incorporated to dynamically update the detection threshold. In this update process, the oldest similarity value is discarded to preserve a reference buffer with a constant number of entries (e.g., 62 for ETTh2, 82 for Consumption and 100 for NI) that is consistent with the number of samples employed during the offline phase to determine the fixed threshold. Figure 9 contrasts the dynamic threshold (bottom) with the fixed threshold (top) using the same subsample length across the three test datasets, where ETTh2 and Consumption are evaluated with TimeGPT and NI is evaluated with TimesFM. The details of detection results are shown in Table 12. Across all datasets, the online detection performance improves significantly when using the dynamic threshold. Specifically, the FAR decreases by approximately 1% for both the ETTh2 and Consumption datasets compared

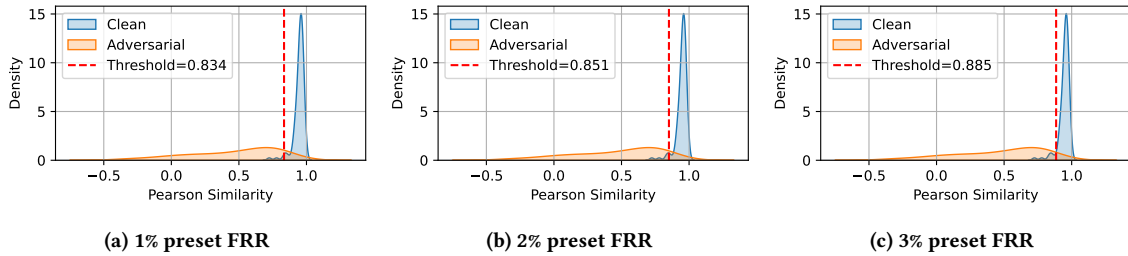


Figure 8: The online similarity distribution at different preset FRR tolerances (ETTh2 dataset on TimesFM). It shows that there is a trade-off between FRR and FAR.

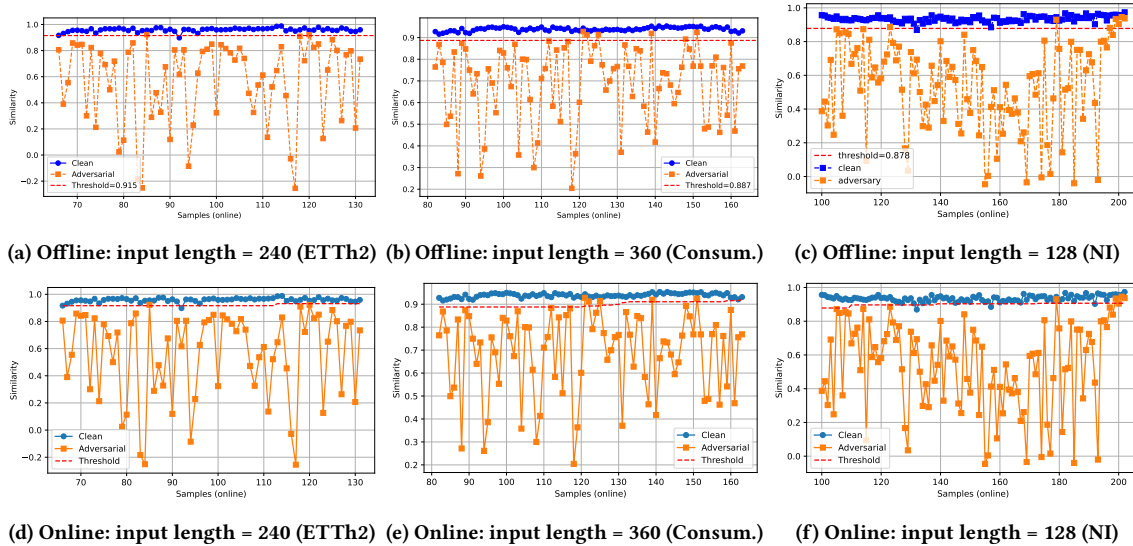


Figure 9: Online fixed threshold (top) and dynamic threshold (bottom) detection results for across different datasets.

Table 12: Detection performance w/wo dynamic threshold.

Dataset	Length	Fixed Thr.	Fixed threshold		Dynamic threshold	
			FRR	FAR	FRR	FAR
ETTh2	240	0.915	1.5%	3.0%	1.5%	1.5%
Consumption	360	0.887	0.0%	7.3%	0.0%	6.1%
NI	128	0.878	1.0%	6.8%	2.9%	3.9%

to the fixed threshold, while the FRR remains unchanged. For the NI dataset, the FAR is reduced by around 2%, although this has a slight increase of online FRR when using the dynamic threshold instead of the fixed one. In summary, dynamic threshold can always achieve a better balance between online FRR and FAR than that of the fixed threshold, while the fixed threshold is easier to use.

6.3 Similarity Metric

In our previous experiments, Pearson similarity was used as the similarity metric. Nonetheless, ILID is independent of the choice of similarity metric. Here, we evaluate ILID using Euclidean distance [36] and Manhattan distance [62], each transformed into a similarity measure as $\text{similarity} = 1/(1 + \text{distance})$. This simple transformation is to make sure the metric value range is between 0 and 1 for facilitating visualized presentation. TimesFM is used as the TS-LLM with the NI dataset. Each sample contains 256 timesteps, and the subsample length is set to 128 by selecting either the odd

Table 13: Detection performance with different similarity metrics (NI on TimesFM).

Metric	Threshold	# of Offline		# of Online	
		FRR	FAR	FRR	FAR
Pearson	0.878	1.0%	1.0%	1.0%	6.8%
Euclidean	0.591	1.0%	0.0%	1.0%	
Manhattan	0.186	1.0%	0.0%	1.0%	

or even elements. Based on the same offline preset FRR of 1.0%, the thresholds are 0.591 for the Euclidean similarity metric and 0.186 for the Manhattan similarity metric. These thresholds are then applied for detection in the online phase. For both similarity metrics, the online FRR for clean samples is 0% and the FAR for adversarial samples is 1.0%, as shown in Figure 10b and Figure 10c. These results are not inferior to those obtained using the Pearson similarity metric, where the online FRR was 1.0% and the FAR was 6.8%, as shown in Figure 10a. Further details are presented in Table 13.

6.4 Evaded Adversarial Examples

We further analyze the adversarial examples that evade ILID, namely those falsely accepted as benign. Our hypothesis is that many of these adversarial inputs may in fact be ineffective, behaving similarly to their clean counterparts. To validate this, we compare the forecasting performance of each undetected adversarial sample

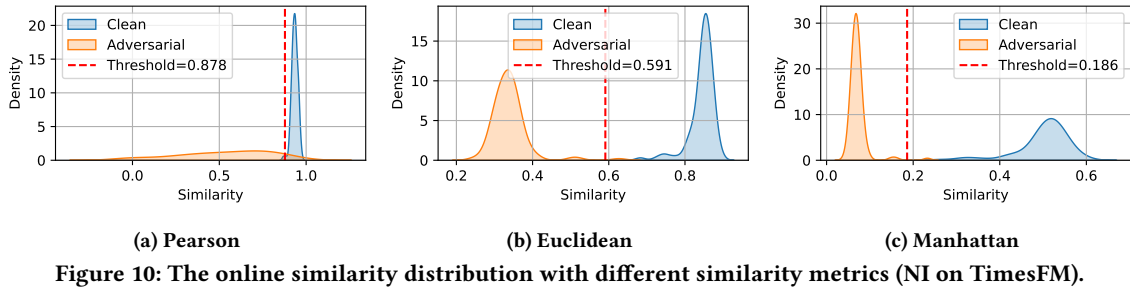


Figure 10: The online similarity distribution with different similarity metrics (NI on TimesFM).

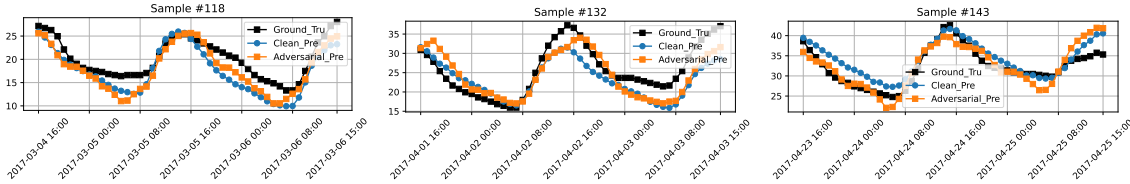


Figure 11: The forecasting between undetected adversarial sample and the corresponding clean sample (ETTh2 on TimesFM).

Table 14: Forecasting performance on evaded samples.

Models	Datasets	Sample Index	Clean query		AE query	
			MAE	MSE	MAE	MSE
TimesFM	NI	123	0.298	0.119	0.270	0.104
		197	0.486	0.311	0.693	0.588
		199	0.917	1.314	0.914	1.214
		200	0.406	0.224	1.245	1.773
		201	0.169	0.040	0.453	0.235
		202	0.686	0.676	1.277	1.832
TimesFM	ETTh2	109	0.385	0.205	0.822	0.745
		110	0.357	0.199	0.467	0.357
		118	0.232	0.070	0.192	0.049
		132	0.314	0.134	0.280	0.101
		134	0.169	0.040	0.453	0.235
		143	0.179	0.047	0.162	0.045
TimeLLM	Consum.	150	0.328	0.171	0.420	0.309
		143	0.219	0.074	0.399	0.188
		182	0.309	0.148	0.442	0.312
		100	0.241	0.085	0.228	0.085
		104	0.320	0.134	0.340	0.225
		110	0.206	0.067	0.281	0.129
TimeLLM	Consum.	134	0.777	0.751	0.657	0.751
		142	0.604	0.399	0.659	0.587
		180	0.275	0.108	0.454	0.299

with its corresponding clean sample. Across datasets, a notable portion of these adversarial examples show no observable attack impact. Table 14 presents the results for the NI and ETTh2 datasets under TimesFM, and the Consumption dataset under TimeLLM. In these tables, blue-highlighted values indicate adversarial samples whose MAE and MSE are equal to or even lower than those of their clean counterparts, providing no evidence of a successful attack. Concretely, for the NI dataset, 2 of 9 samples (#123 and #129; 22.2%) show no attack effect. For the ETTh2 dataset, 3 of 9 samples (#118, #132, and #143; 33.4%) are similarly ineffective. For the Consumption dataset, 2 of 6 samples (#100 and #134; 33.4%) exhibit no measurable attack. In summary, approximately 30% of the adversarial examples that bypass ILID do so not because they succeed, but because they fail to introduce any meaningful perturbation. This is further illustrated in Figure 11, where three such

Table 15: Exchange Rate forecasting performance w/wo attack on TimeLLM.

Dataset	Target	Clean query			AE query		
		MAE	MSE	R ²	MAE	MSE	R ²
Exchange Rate	Australia	0.125	0.030	96.2%	0.396	0.228	71.0%

Table 16: Detection performance with Exchange Rate on TimeLLM.

Dataset	Length	Threshold	Offline			Online		
			FRR	FRR	FAR	FRR	FAR	
Exchange Rate	56	0.907	1.0%	2.9%	2.9%			

ETTh2 samples (#118, #132, #143) clearly demonstrate negligible deviation from their clean counterparts.

6.5 Broader Application of Forecasting

Here, we show that ILID extends effectively beyond energy-related forecasting tasks. Using the Currency Exchange Rate dataset, which contains daily USD exchange rates for eight countries from 1990 to 2016 [32], we evaluate ILID on a financial forecasting scenario. The experiment uses the USD-to-AUD series, where an adversarial attack is applied to a TimeLLM model forecasting the next 12 steps based on the past 168 timesteps. Table 15 reports the forecasting performance with and without attack. Among the 239 total samples, the first 100 are used to determine an offline threshold of 0.907 with a preset FRR of 1% and a subsample length of 56. As shown in Table 16, the resulting online FRR and FAR are both 2.9%. Together, these results highlight the broad applicability and strong generalization ability of ILID across diverse domains, including financial time-series forecasting.

7 Conclusion

This work has proposed ILID, which leverages the unique input length independence of TS-LLMs to detect adversarial inputs. Importantly, ILID operates without modifying the underlying TS-LLM,

functioning instead as a plug-in module that can be seamlessly integrated with TS-LLMs. Extensive experiments on three energy-specific datasets across three TS-LLMs (including both proprietary and open-source models) demonstrate the efficiency and effectiveness of ILID in detecting adversarial inputs, under both the latest black-box attacks and well-established white-box attacks. Notably, due to its inherent randomness, ILID exhibits strong resilience against adaptive attacks; in particular, we demonstrate its effectiveness against a sparse adversarial example attack. Extending and validating ILID in other forecasting domains, such as finance, as well as across different modalities, represents a promising direction for future research. This potential lies in the broader fact that foundation models, including LLMs and VLMs, are inherently capable of handling inputs of varying lengths.

Ethical Considerations

This work investigates adversarial vulnerabilities in TS-LLMs used for energy forecasting, a domain connected to critical infrastructure. All experiments rely solely on publicly available, non-sensitive datasets, and no operational systems or private information were accessed. While we evaluate both black-box and white-box attacks, we intentionally provide only the technical details required for reproducibility and do not release exploit code or parameters that could enable misuse.

Acknowledgment

This work is supported by CSIRO – National Science Foundation (US) AI Research Collaboration Program (NSF-2302720-CSIRO of RAIIoE grant).

References

- [1] [n. d.]. *Hourly Energy Consumption*. <https://www.kaggle.com/datasets/robikscube/hourly-energy-consumption>
- [2] [n. d.]. *Hourly Energy Consumption and Production*. <https://www.kaggle.com/datasets/stefancomanita/hourly-electricity-consumption-and-production>
- [3] Ghadeer O Alsharif, Christos Anagnostopoulos, and Angelos K Marnerides. 2025. Energy Market Manipulation via False-Data Injection Attacks. *IEEE Access* (2025).
- [4] Abdul Fatir Ansari, Lorenzo Stella, Caner Turkmen, Xiyuan Zhang, Pedro Mercado, Huibin Shen, Oleksandr Shchur, Syama Sundar Rangapuram, Sebastian Pineda Arango, Shubham Kapoor, et al. 2024. Chronos: Learning the language of time series. *arXiv preprint arXiv:2403.07815* (2024).
- [5] Anomadarshi Barua and Mohammad Abdullah Al Faruque. 2020. Hall Spoofing: A {Non-Invasive} {DoS} Attack on {Grid-Tied} Solar Inverter. In *29th USENIX Security Symposium (USENIX Security 20)*. 1273–1290.
- [6] Dmitriy Beshpalov, Sourav Bhabesh, Yi Xiang, Liutong Zhou, and Yanjun Qi. 2024. Towards building a robust toxicity predictor. *arXiv preprint arXiv:2404.08690* (2024).
- [7] Defu Cao, Furong Jia, Sercan O Arik, Tomas Pfister, Yixiang Zheng, Wen Ye, and Yan Liu. 2023. Tempo: Prompt-based generative pre-trained transformer for time series forecasting. *arXiv preprint arXiv:2310.04948* (2023).
- [8] Nicholas Carlini and David Wagner. 2017. Magnet and efficient defenses against adversarial attacks* are not robust to adversarial examples. *arXiv preprint arXiv:1711.08478* (2017).
- [9] Ching Chang, Wen-Chih Peng, and Tien-Fu Chen. 2023. Llm4ts: Two-stage fine-tuning for time-series forecasting with pre-trained llms. *CoRR* (2023).
- [10] Raphaël Dang-Nhu, Gagandeep Singh, Pavol Bielik, and Martin Vechev. 2020. Adversarial attacks on probabilistic autoregressive forecasting models. In *International Conference on Machine Learning*. PMLR, 2356–2365.
- [11] Abhimanyu Das, Weihao Kong, Rajat Sen, and Yichen Zhou. 2024. A decoder-only foundation model for time-series forecasting. In *Forty-first International Conference on Machine Learning*.
- [12] Fanidhar Dewangan, Almoataz Y Abdelaziz, and Monalisa Biswal. 2023. Load forecasting models in smart grid using smart meter information: A review. *Energies* 16, 3 (2023), 1404.
- [13] Ashkan Entezari, Alireza Aslani, Rahim Zahedi, and Younes Noorollahi. 2023. Artificial intelligence and machine learning in energy systems: A bibliographic perspective. *Energy Strategy Reviews* 45 (2023), 101017.
- [14] Hassan Ismail Fawaz, Germain Forestier, Jonathan Weber, Lhassane Idoumghar, and Pierre-Alain Muller. 2019. Adversarial attacks on deep neural networks for time series classification. In *2019 International joint conference on neural networks (IJCNN)*. IEEE, 1–8.
- [15] Yansong Gao, Seyit A Camtepe, Nazatul Haque Sultan, Hang Thanh Bui, Arash Mahboubi, Hamed Aboutorab, Michael Bewong, Rafiqul Islam, Md Zahidul Islam, Afeef Chauhan, et al. 2024. Security threats to agricultural artificial intelligence: Position and perspective. *Computers and Electronics in Agriculture* 227 (2024), 109557.
- [16] Azul Garza, Cristian Challu, and Max Mergenthaler-Canseco. 2023. TimeGPT-1. *arXiv preprint arXiv:2310.03589* (2023).
- [17] Gregor Giebel, Richard Brownsword, George Kariniotakis, Michael Denhard, and Caroline Draxl. 2011. The state-of-the-art in short-term prediction of wind power: A literature overview.
- [18] Ian J Goodfellow, Jonathon Shlens, and Christian Szegedy. 2014. Explaining and harnessing adversarial examples. *arXiv preprint arXiv:1412.6572* (2014).
- [19] Yuvaraj Govindarajulu, Avinash Amballa, Pavan Kulkarni, and Manojkumar Parmar. 2023. Targeted attacks on timeseries forecasting. *arXiv preprint arXiv:2301.11544* (2023).
- [20] Kathrin Grosse, Praveen Manoharan, Nicolas Papernot, Michael Backes, and Patrick McDaniel. 2017. On the (statistical) detection of adversarial examples. *arXiv preprint arXiv:1702.06280* (2017).
- [21] Nate Gruver, Marc Finzi, Shikai Qiu, and Andrew G Wilson. 2023. Large language models are zero-shot time series forecasters. *Advances in Neural Information Processing Systems* 36 (2023), 19622–19635.
- [22] Chuan Guo, Mayank Rana, Moustapha Cisse, and Laurens van der Maaten. 2017. Countering adversarial images using input transformations. *arXiv preprint arXiv:1711.00117* (2017).
- [23] Chih-Hui Ho and Nuno Vasconcelos. 2022. DISCO: Adversarial defense with local implicit functions. *Advances in Neural Information Processing Systems* 35 (2022), 23818–23837.
- [24] Chenghao Huang, Siyang Li, Ruohong Liu, Hao Wang, and Yize Chen. 2024. Large foundation models for power systems. In *2024 IEEE Power & Energy Society General Meeting (PESGM)*. IEEE, 1–5.
- [25] Xiangyu Hui, Samuel Karumba, Sid Chi-Kin Chau, and Mohiuddin Ahmed. 2025. Destabilizing Power Grid and Energy Market by Cyberattacks on Smart Inverters (*E-Energy '25*). Association for Computing Machinery, 136–151. <https://doi.org/10.1145/3679240.3734613>
- [26] Yushan Jiang, Zijie Pan, Xikun Zhang, Sahil Garg, Anderson Schneider, Yuriy Nevmyvaka, and Dongjin Song. 2024. Empowering time series analysis with large language models: A survey. *arXiv preprint arXiv:2402.03182* (2024).
- [27] Ming Jin, Shiyu Wang, Lintao Ma, Zhixuan Chu, James Y Zhang, Xiaoming Shi, Pin-Yu Chen, Yuxuan Liang, Yuan-Fang Li, Shirui Pan, et al. 2023. Time-llm: Time series forecasting by reprogramming large language models. *arXiv preprint arXiv:2310.01728* (2023).
- [28] Ming Jin, Qingsong Wen, Yuxuan Liang, Chaoli Zhang, Siqiao Xue, Xue Wang, James Zhang, Yi Wang, Haifeng Chen, Xiaoli Li, et al. 2023. Large models for time series and spatio-temporal data: A survey and outlook. *arXiv preprint arXiv:2310.10196* (2023).
- [29] Fazle Karim, Somshubra Majumdar, and Houshang Darabi. 2020. Adversarial attacks on time series. *IEEE transactions on pattern analysis and machine intelligence* 43, 10 (2020), 3309–3320.
- [30] Aounon Kumar, Chirag Agarwal, Suraj Srinivas, Aaron Jiaxun Li, Soheil Feizi, and Himabindu Lakkaraju. 2023. Certifying llm safety against adversarial prompting. *arXiv preprint arXiv:2309.02705* (2023).
- [31] Alexey Kurakin, Ian J Goodfellow, and Samy Bengio. 2018. Adversarial examples in the physical world. In *Artificial intelligence safety and security*. Chapman and Hall/CRC, 99–112.
- [32] Guokun Lai, Wei-Cheng Chang, Yiming Yang, and Hanxiao Liu. 2018. Modeling long- and short-term temporal patterns with deep neural networks. In *The 41st international ACM SIGIR conference on research & development in information retrieval*. 95–104.
- [33] Jinze Li, Jinfeng Xu, Shuo Yang, and Edith CH Ngai. 2024. Large Language Models in Smart Grid: Applications and Risks. In *International Conference on Smart Grid Inspired Future Technologies*. Springer, 3–19.
- [34] Min Liang, Yongli Hu, Haoen Weng, Jiayang Xi, and Baocai Yin. 2025. EnergyGPT: Fine-tuning large language model for multi-energy load forecasting. *Renewable Energy* (2025), 123313.
- [35] Yuxuan Liang, Haomin Wen, Yuqi Nie, Yushan Jiang, Ming Jin, Dongjin Song, Shirui Pan, and Qingsong Wen. 2024. Foundation models for time series analysis: A tutorial and survey. In *Proceedings of the 30th ACM SIGKDD conference on knowledge discovery and data mining*. 6555–6565.
- [36] Jason Lines, Luke M Davis, Jon Hills, and Anthony Bagnall. 2012. A shapelet transform for time series classification. In *Proceedings of the 18th ACM SIGKDD international conference on Knowledge discovery and data mining*. 289–297.

- [37] Chenxi Liu, Qianxiong Xu, Hao Miao, Sun Yang, Lingzheng Zhang, Cheng Long, Ziyue Li, and Rui Zhao. 2025. Timecma: Towards llm-empowered multivariate time series forecasting via cross-modality alignment. In *Proceedings of the AAAI Conference on Artificial Intelligence*, Vol. 39. 18780–18788.
- [38] Fuqiang Liu and Sicong Jiang. 2025. Temporally Sparse Attack for Fooling Large Language Models in Time Series Forecasting. (2025).
- [39] Fuqiang Liu, Sicong Jiang, Luis Miranda-Moreno, Seongjin Choi, and Lijun Sun. 2025. Adversarial Vulnerabilities in Large Language Models for Time Series Forecasting. In *International Conference on Artificial Intelligence and Statistics (AISTATS)*.
- [40] Peiyuan Liu, Hang Guo, Tao Dai, Naiqi Li, Jigang Bao, Xudong Ren, Yong Jiang, and Shu-Tao Xia. 2025. Calf: Aligning llms for time series forecasting via cross-modal fine-tuning. In *Proceedings of the AAAI Conference on Artificial Intelligence*, Vol. 39. 18915–18923.
- [41] Zihao Liu, Qi Liu, Tao Liu, Nuo Xu, Xue Lin, Yanzhi Wang, and Wujie Wen. 2019. Feature distillation: Dnn-oriented jpeg compression against adversarial examples. In *2019 IEEE/CVF Conference on Computer Vision and Pattern Recognition (CVPR)*. IEEE, 860–868.
- [42] Shiqing Ma, Yingqi Liu, Guan hong Tao, Wen-Chuan Lee, and Xiangyu Zhang. 2019. NIC: Detecting Adversarial Samples with Neural Network Invariant Checking. In *NDSS*.
- [43] Xingjun Ma, Bo Li, Yisen Wang, Sarah M Erfani, Sudanthi Wijewickrema, Grant Schoenebeck, Dawn Song, Michael E Houle, and James Bailey. 2018. Characterizing adversarial subspaces using local intrinsic dimensionality. In *International Conference on Learning Representations (ICLR)*.
- [44] Aleksander Madry, Aleksandar Makelov, Ludwig Schmidt, Dimitris Tsipras, and Adrian Vladu. 2018. Towards deep learning models resistant to adversarial attacks. In *ICLR*.
- [45] Izaskun Oregi, Javier Del Ser, Aritz Perez, and Jose A Lozano. 2018. Adversarial sample crafting for time series classification with elastic similarity measures. In *International Symposium on Intelligent and Distributed Computing*. Springer, 26–39.
- [46] Nicolas Papernot, Patrick McDaniel, and Ian Goodfellow. 2016. Transferability in machine learning: from phenomena to black-box attacks using adversarial samples. *arXiv preprint arXiv:1605.07277* (2016).
- [47] Nicolas Papernot, Patrick McDaniel, Somen Jha, Matt Fredrikson, Z Berkay Celik, and Ananthram Swami. 2016. The limitations of deep learning in adversarial settings. In *2016 IEEE European symposium on security and privacy (EuroS&P)*. IEEE, 372–387.
- [48] Mansi Phute, Alec Helbling, Matthew Hull, ShengYun Peng, Sebastian Szyller, Cory Cornelius, and Duen Horng Chau. 2023. Llm self defense: By self examination, llms know they are being tricked. *arXiv preprint arXiv:2308.07308* (2023).
- [49] Pierre Pinson. 2013. Wind energy: Forecasting challenges for its operational management. *Statist. Sci.* (2013).
- [50] Dawei Qiu, Jianhong Wang, Guangchun Ruan, Qianzhi Zhang, and Goran Strbac. 2024. Robust Reinforcement Learning for Decision Making Under Uncertainty in Electricity Markets. *IEEE Transactions on Power Systems* (2024).
- [51] Kashif Rasul, Arjun Ashok, Andrew Robert Williams, Arian Khorasani, George Adamopoulos, Rishika Bhagwatkar, Marin Biloš, Hena Ghonia, Nadhir Hassen, Anderson Schneider, et al. 2023. Lag-llama: Towards foundation models for time series forecasting. In *RO-FoMo: Robustness of Few-shot and Zero-shot Learning in Large Foundation Models*.
- [52] Pradeep Rathore, Arghya Basak, Sri Harsha Nistala, and Venkataramana Runkana. 2020. Untargeted, targeted and universal adversarial attacks and defenses on time series. In *2020 international joint conference on neural networks (IJCNN)*. IEEE, 1–8.
- [53] Muhammad Qamar Raza and Abbas Khosravi. 2015. A review on artificial intelligence based load demand forecasting techniques for smart grid and buildings. *Renewable and Sustainable Energy Reviews* 50 (2015), 1352–1372.
- [54] Bushra Sabir, M Ali Babar, and Sharif Abuadbbba. 2023. Interpretability and transparency-driven detection and transformation of textual adversarial examples (it-dt). *arXiv preprint arXiv:2307.01225* (2023).
- [55] Manuela Sanguinetti and Maurizio Atzori. 2024. Conversational agents for energy awareness and efficiency: A survey. *Electronics* 13, 2 (2024), 401.
- [56] Sayantan Sarker, Ankan Bansal, Upal Mahbub, and Rama Chellappa. 2017. UP-SET and ANGR: Breaking high performance image classifiers. *arXiv preprint arXiv:1707.01159* (2017).
- [57] Nikan Shahverdi, Arina Saffari, and Babak Amiri. 2025. A systematic review of artificial intelligence and machine learning in energy sustainability: Research topics and trends. *Energy Reports* 13 (2025), 5551–5578.
- [58] Jiawei Su, Danilo Vasconcellos Vargas, and Kouichi Sakurai. 2019. One pixel attack for fooling deep neural networks. *IEEE Transactions on Evolutionary Computation* (2019).
- [59] Chenxi Sun, Hongyan Li, Yaliang Li, and Shenda Hong. 2023. Test: Text prototype aligned embedding to activate llm’s ability for time series. *arXiv preprint arXiv:2308.08241* (2023).
- [60] Christian Szegedy, Wojciech Zaremba, Ilya Sutskever, Joan Bruna, Dumitru Erhan, Ian Goodfellow, and Rob Fergus. 2013. Intriguing properties of neural networks. *arXiv preprint arXiv:1312.6199* (2013).
- [61] Mingting Tan, Mike Merrill, Vinayak Gupta, Tim Althoff, and Tom Hartvigsen. 2024. Are language models actually useful for time series forecasting? *Advances in Neural Information Processing Systems* 37 (2024), 60162–60191.
- [62] Xiaoyue Wang, Abdullah Mueen, Hui Ding, Goce Trajcevski, Peter Scheuermann, and Eamonn Keogh. 2013. Experimental comparison of representation methods and distance measures for time series data. *Data Mining and Knowledge Discovery* 26, 2 (2013), 275–309.
- [63] Yuchen Wang, Xiaoguang Li, Li Yang, Jianfeng Ma, and Hui Li. 2023. ADDITION: Detecting Adversarial Examples With Image-Dependent Noise Reduction. *IEEE Transactions on Dependable and Secure Computing* (2023).
- [64] Zeyu Wang, Xianhang Li, Hongru Zhu, and Cihang Xie. 2024. Revisiting adversarial training at scale. In *Proceedings of the IEEE/CVF Conference on Computer Vision and Pattern Recognition*. 24675–24685.
- [65] Carissa Wong. 2024. How AI is improving climate forecasts. *Nature* 628, 8009 (2024), 710–712.
- [66] Gerald Woo, Chenghao Liu, Akshat Kumar, Caiming Xiong, Silvio Savarese, and Doyen Sahoo. 2024. Unified training of universal time series forecasting transformers. (2024).
- [67] Tao Wu, Xuechun Wang, Shaojie Qiao, Xingping Xian, Yanbing Liu, and Liang Zhang. 2022. Small perturbations are enough: Adversarial attacks on time series prediction. *Information Sciences* 587 (2022), 794–812.
- [68] Lei Xu, Yangyi Chen, Ganqu Cui, Hongcheng Gao, and Zhiyuan Liu. 2022. Exploring the universal vulnerability of prompt-based learning paradigm. *arXiv preprint arXiv:2204.05239* (2022).
- [69] Weilin Xu, David Evans, and Yanjun Qi. 2017. Feature squeezing: Detecting adversarial examples in deep neural networks. *arXiv preprint arXiv:1704.01155* (2017).
- [70] Hao Xue and Flora D Salim. 2023. Promptcast: A new prompt-based learning paradigm for time series forecasting. *IEEE Transactions on Knowledge and Data Engineering* 36, 11 (2023), 6851–6864.
- [71] Minhui Xue, Surya Nepal, Ling Liu, Subbu Sethuvenkatraman, Xingliang Yuan, Carsten Rudolph, Ruoxi Sun, and Greg Eisenhauer. 2023. RAI4IoE: Responsible AI for enabling the Internet of Energy. In *2023 5th IEEE International Conference on Trust, Privacy and Security in Intelligent Systems and Applications (TPS-ISA)*. IEEE, 13–22.
- [72] Fengchen Yang, Zihao Dan, Kaikai Pan, Chen Yan, Xiaoyu Ji, and Wenyuan Xu. 2025. Rethink: Reveal the threat of electromagnetic interference on power inverters. *NDSS* (2025).
- [73] Shigeng Zhang, Shuxin Chen, Chengyao Hua, Zhetao Li, Yanchun Li, Xuan Liu, Kai Chen, Zhankai Li, and Weiping Wang. 2023. LSD: Adversarial Examples Detection Based on Label Sequences Discrepancy. *IEEE Transactions on Information Forensics and Security* (2023).
- [74] Xinyu Zhang, Hanbin Hong, Yuan Hong, Peng Huang, Binghui Wang, Zhongjie Ba, and Kui Ren. 2024. Text-crs: A generalized certified robustness framework against textual adversarial attacks. In *2024 IEEE Symposium on Security and Privacy (SP)*. IEEE, 2920–2938.
- [75] Dawei Zhou, Yukun Chen, Nannan Wang, Decheng Liu, Xinbo Gao, and Tongliang Liu. 2023. Eliminating adversarial noise via information discard and robust representation restoration. In *International Conference on Machine Learning*. PMLR, 42517–42530.
- [76] Haoyi Zhou, Shanghang Zhang, Jieqi Peng, Shuai Zhang, Jianxin Li, Hui Xiong, and Wancai Zhang. 2021. Informer: Beyond efficient transformer for long sequence time-series forecasting. In *Proceedings of the AAAI conference on artificial intelligence*, Vol. 35. 11106–11115.
- [77] Tian Zhou, Peisong Niu, Liang Sun, Rong Jin, et al. 2023. One fits all: Power general time series analysis by pretrained lm. *Advances in neural information processing systems* 36 (2023), 43322–43355.